

# First light on the DiPOLE project

Contact [s.banerjee@stfc.ac.uk](mailto:s.banerjee@stfc.ac.uk)

## S. Banerjee

STFC, Central Laser Facility

## K. Ertel

STFC, Central Laser Facility

## P. Mason

STFC, Central Laser Facility

## P.J. Phillips

STFC, Central Laser Facility

## S. Tomlinson

STFC, Central Laser Facility

## S. Blake

STFC, Central Laser Facility

## J. Greenhalgh

STFC, Central Laser Facility

## Introduction

We report on the first demonstration of a diode pumped, gas cooled, cryogenic multi-slab Yb:YAG amplifier. The performance was characterised over a temperature range from 88 K to 175 K. A maximum small-signal single-pass longitudinal gain of 11.0 was measured at 88 K. When amplifying ns-pulses, recorded output energies were 10.1 J at 1 Hz in a 4-pass extraction geometry and 6.4 J at 10 Hz in a 3-pass setup, corresponding to optical-to-optical conversion efficiencies of 21 % and 16 %, respectively. To our knowledge, this represents the highest pulse energy so far obtained from a cryo-cooled Yb-laser and the highest efficiency from a multi-J DPSSL system.

## Introduction

Multi-J to kJ-class lasers are pivotal to the advancement of ultra-high intensity laser-matter interaction studies such as particle acceleration, intense X-ray generation and inertial confinement fusion. If operated at high repetition rate and high overall efficiency, these lasers offer the potential for development of viable real-world applications. For example, inertial fusion energy production which is under investigation in the HiPER project, or to generate ultra-short, ultra-bright sources of radiation and particles, in projects such as the Extreme Light Infrastructure (ELI). Current kJ-class laser facilities like the National Ignition Facility (NIF) rely on flashlamp pumped Nd:Glass technology, which exhibits very poor electrical-to-optical efficiency and can only be operated at very low repetition rates (few shots per day). Therefore, a new approach in the form of diode pumped solid state laser (DPSSL) systems, using advanced gain media and cooling schemes, is required to overcome these limitations. Current and previous high-energy DPSSL development projects include Mercury with average power and efficiency values of 550 W and 7.6 % [1], LUCIA with 20 W and 5.7 % [2], HALNA with 213 W and 11.7 % [3], and Polaris with 1.2 W and 6 % [4]. In the last annual report we have presented our conceptual design of a scalable diode pumped, gas cooled, cryogenic multi-slab Yb:YAG amplifier [5], capable of generating kJ-class pulse energies. In order to demonstrate the viability of this concept, a scaled-down prototype, DiPOLE (Diode Pumped Optical Laser

## A. Lintern

STFC, Engineering Technology Centre

## T. Davenne

STFC, Engineering Technology Centre

## M. Fitton

STFC, Engineering Technology Centre

## J. Collier

STFC, CLF

Experiment), is currently under development. In this paper, we present first results obtained over a temperature range from 88 K to 175 K.

## Experiment setup and results

Figure 1 shows a schematic diagram of the DiPOLE system. A Yb:CaF<sub>2</sub> cavity-dumped oscillator, tuneable from 1025 nm to 1040 nm with a spectral bandwidth of 0.2 nm, was used as the seed source, delivering up to 180  $\mu$ J at 1030 nm and 10 Hz in a 10 ns (FWHM) pulse duration. The oscillator output was expanded to a 2 mm diameter beam and further amplified by a thin-disk Yb:YAG multi-pass pre-amplifier. This consisted of a 2 mm thick, 2.5 at.% doped Yb:YAG crystal arranged in an active mirror configuration, which was pulse pumped by a 940 nm, 2 kW peak power, diode stack for 1 ms duration. An image-relaying multi-pass architecture, reported earlier [6] was used to double-pass the gain medium 7 times. The pre-amplifier

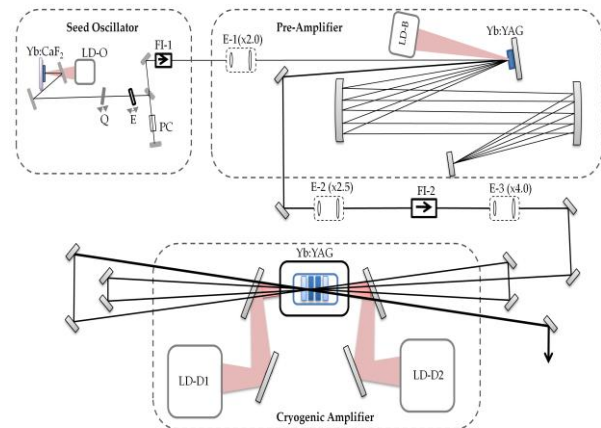
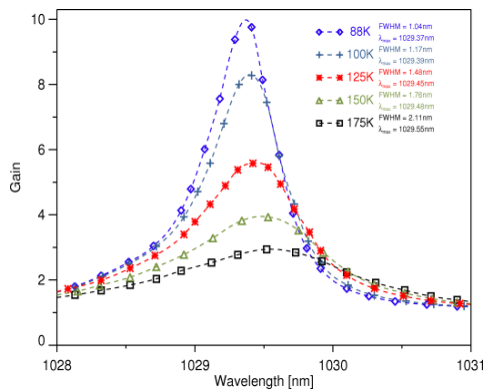


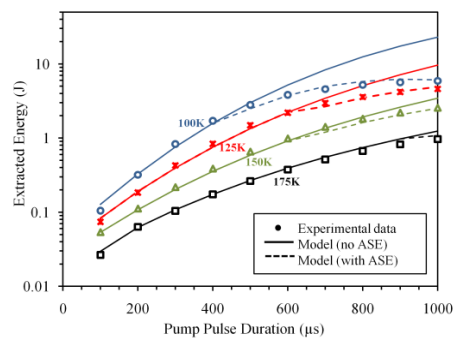
Figure 1: Schematic diagram of the DiPOLE system.

The DiPOLE main amplifier head contained four ceramic YAG discs (Konoshima) each with a diameter of 55 mm and a thickness of 5 mm. The discs consisted of a 35 mm diameter Yb-doped inner region that is surrounded by a 10 mm wide Cr<sup>4+</sup>-doped cladding to minimise ASE loss and prevent parasitic oscillations at high gain. The inner two discs had a higher Yb doping of 2.0 at.% than the outer two discs at 1.1 at.%. Thickness and doping levels were chosen to maximise optical efficiency whilst maintaining an acceptable level of ASE loss at the amplifier's design temperature of 175 K [7]. The discs were held in aerodynamically shaped vanes and arranged in a stack with 1.5 mm gaps in-between discs. Helium gas at cryogenic temperature was forced through the gaps at a typical volume flow rate of 35 m<sup>3</sup>/h and pressure of 10 bar. The helium gas was cooled by passing it through a liquid nitrogen heat exchanger and circulated by a cryogenic fan (Cryozone). The amplifier was pumped from both sides by two 940 nm diode laser sources (Ingeneric, Jenoptik and Amtron) each delivering 20 kW peak power with variable pulse duration up to 1.2 ms and repetition rate up to 10 Hz. The emission spectrum of the diode sources was less than 6 nm (FWHM) wide. The pump sources produced a 20x20 mm<sup>2</sup> square, flat-top beam profile at their image plane, which was arranged to lie at the centre of the amplifier head. A low power cw external cavity tuneable diode laser (ECDL) (Sacher TEC520), was employed for small-signal gain measurements of the DiPOLE amplifier. Figure 2 shows the wavelength dependence of the measured single-pass, small-signal gain for different operating temperatures when pumped for 1 ms at 10 Hz and 40 kW peak power. The gain increased with decreasing temperature, owing to the increase in emission cross-section. A maximum small-signal single-pass gain of 9.8 was recorded at 88 K, increasing to 11.0 for 1.2 ms pump duration. However, this was accompanied by a reduction in gain bandwidth to 1.04 nm (FWHM) at 88 K, approximately half the value measured at 175 K, along with a blue shift of the peak gain wavelength by 0.18 nm.



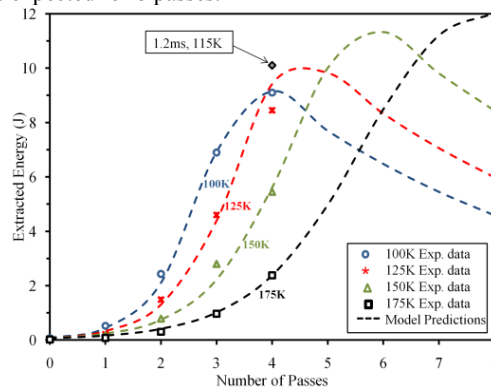
**Figure 2: Small-signal single-pass gain for the main amplifier at different temperatures measured at 10 Hz and 1 ms pump duration.**

For ns-pulse amplification studies, the main amplifier was seeded by the pulsed output from the pre-amplifier. The circular beam was expanded to overflow the 20x20 mm<sup>2</sup> square pumped region within the amplifier, the energy after beam expansion was approximately 60 mJ. A simple bow-tie arrangement was then installed to pass the seed beam through the amplifier up to 4 times, as shown in Figure 1. Figure 3 shows the measured output energy for different operating temperatures as a function of pump pulse duration for a 3-pass configuration. Numerical model predictions with and without the inclusion of ASE losses are also shown. The performance of the system was modelled as described in [7] along with empirically derived ASE loss values.



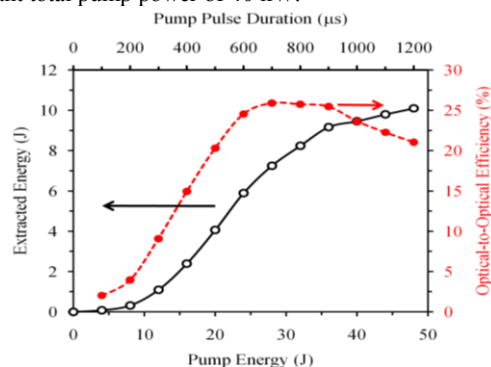
**Figure 3: Extracted energy as a function of pump pulse duration measured at different temperatures for 1 Hz operation in a 3-pass configuration.**

Figure 4 shows the predicted output energy as a function of the number of extraction passes for a pump duration of 1 ms. Experimental values for extracted energy measured for up to 4 passes, at different temperatures and at 1 Hz repetition rate, are also included in the graph. At 100 K, the maximum energy predicted and observed was clamped at 9.1 J in a 4-pass configuration owing to increased ASE losses. However, at the higher design temperature of 175 K, pulse energy as high as 12 J is expected for 8 passes.



**Figure 4: Predicted output energy of the DiPOLE amplifier for 8 passes along with the experimental values measured for up to 4 passes at different temperatures for 1 Hz operation and 1 ms pump pulse duration.**

In a separate experiment with the pump pulse duration increased to 1.2 ms, the amplifier delivered 10.1 J at 115 K with a repetition rate of 1 Hz, which corresponds to an optical-to-optical efficiency ( $\eta_{o-o}$ ) of 21%. Figure 5 shows extracted pulse energy and  $\eta_{o-o}$  as a function of pump energy. Here the amplifier was operated in a 4-pass configuration and the pump energy was varied by changing the pump pulse duration at constant total pump power of 40 kW.



**Figure 5: Extracted pulse energy (solid line) and  $\eta_{o-o}$  (dotted line) of the DiPOLE amplifier for up to 1.2 ms pump pulse duration at 1 Hz, 4-passes and 115 K coolant temperature.**

Figure 6 compares the output energy from the amplifier at 1 Hz and 10 Hz pulse repetition rates for a 3-pass extraction setup over a range of operating temperatures and for a fixed pump pulse duration of 1 ms. The dependence of extracted energy on coolant temperature is similar for both 10 Hz and 1 Hz operation, with an offset of approximately 8 K. This offset is believed to be caused by an increase in gain medium temperature due to the additional heat load at 10 Hz operation. This can be compensated by reducing the inlet temperature of the coolant, thus restoring performance to a level similar to that at 1 Hz operation. For 10 Hz operation, the highest pulse energy recorded was 6.4 J, in 3-pass configuration, at a coolant temperature of 93 K. This corresponds to an average power of 64 W and an  $\eta_{o-o}$  of 16%. At this operating temperature, approximately 80 K below the design temperature, output energy and efficiency was limited by ASE loss. A relay-imaging multi-pass extraction architecture, capable of supporting up to 9 passes, is currently being installed. This will increase  $\eta_{o-o}$  by maintaining a better overlap between pump and extraction beams and, more importantly, by enabling operation at higher coolant temperatures with reduced gain and ASE loss.

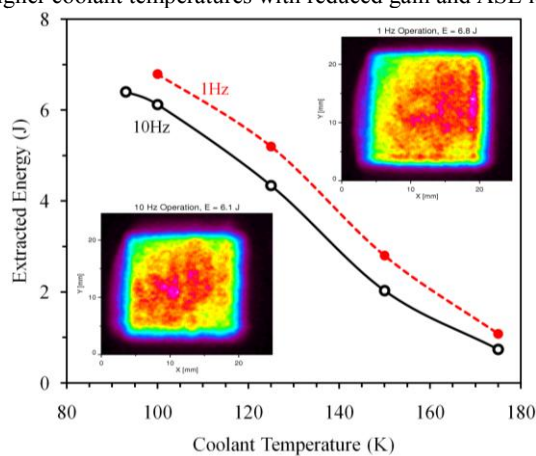


**Figure 6: Extracted energy from the main amplifier at 1 Hz and 10 Hz pulse repetition rates for a 3-pass extraction setup at different temperatures and for fixed pump pulse duration of 1 ms. Inserted are the typical beam profiles for 1 Hz and 10 Hz after the main amplification stage.**

## Conclusions

In summary, we have demonstrated 10.1 J at 1 Hz (4-pass) and 6.4 J at 10 Hz (3-pass) from a diode pumped, gas cooled, cryogenic multi-slab Yb:YAG amplifier with an  $\eta_{o-o}$  of 21% and 16%, respectively. This confirms the viability of multi-slab cryogenic amplifier concept, which is scalability to the kJ level. Further increases in average power to greater than 100 W and optical-to-optical efficiency greater than 25% are expected at the design temperature of 175 K.

## References

1. A. Bayramian, P. Armstrong, E. Ault, R. Beach, C. Bibeau, J. Caird, R. Campbell, B. Chai, J. Dawson, C. Ebbers, A. Erlandson, Y. Fei, B. Freitas, R. Kent, Z. Liao, T. Ladrán, J. Menapace, B. Molander, S. Payne, N. Peterson, M. Randles, K. Schaffers, S. Sutton, J. Tassano, S. Telford, and E. Utterback, *Fusion Sci. Technol.* **52**, 383–387 (2007).
2. D. Albach, M. Arzakantsyan, G. Bourdet, J.-C. Chanteloup, P. Hollander, and B. Vincent, *J. Phys.: Conf. Ser.* **244**, 032015 (2010).
3. R. Yasuhara, T. Kawashima, T. Sekine, T. Kurita, T. Ikegawa, O. Matsumoto, M. Miyamoto, H. Kan, H. Yoshida, J. Kawanaka, M. Nakatsuka, N. Miyanaga, Y. Izawa, and T. Kanabe *Opt. Lett.* **33**, 1711-1713 (2008).
4. J. Hein, S. Podleska, M. Siebold, M. Hellwing, R. Bodefled, R. Sauerbrey, D. Ehrhart, and W. Wintzer, *Appl. Phys. B* **79**, 419 - 422 (2004).

5. P. Mason, K. Ertel, S. Banerjee, P. J. Phillips, J. L. Collier et al, 'Current status of the DiPOLE project' CLF Annual report (2011-2010).
6. M. Siebold, M. Loeser, U. Schramm, J. Koerner, M. Wolf, M. Hellwing, J. Hein, and K. Ertel, *Opt. Express* **17**, 19887–19893 (2009).
7. K. Ertel, S. Banerjee, P. D. Mason, P. J. Phillips, C. Hernandez-Gomez, and J. L. Collier, *Opt. Express* **19**, 26610-26626 (2011).

# Two beam spatial and temporal coherent phasing with femtosecond pulses

Contact [jonathan.phillips@stfc.ac.uk](mailto:jonathan.phillips@stfc.ac.uk)

## Jonathan Phillips

Central Laser Facility  
RAL

## Cristina Hernandez-Gomez

Central Laser Facility  
RAL

## John Collier

Central Laser Facility  
RAL

## Ian Musgrave

Central Laser Facility  
Waseem Shaikh

Central Laser Facility  
RAL

## Introduction

High average powered lasers are attractive owing to their potential for enabling a diverse range of experiments. The power extractable from current laser systems is limited by the size and damage threshold of the amplifying medium or other optical components. Other important additional factors limiting the scale of amplifiers for repetitive systems are ASE, laser material growth, thermal effects and depolarization. An alternative scheme of achieving high power is to combine several beams into a monolithic beam, which immediately reduces the requirements for the amplifier to a more modest level.

## Experiment

We have developed a test bed to investigate a method for spatial recombining and temporal overlap. We have a Ti:Sapphire laser which can produce pulses of  $\sim 200$  fs,  $\sim 5$  nJ of energy per pulse and has a wavelength tuning range of 950-1080 nm at 80 MHz. In these experiments the laser is used in the femtosecond mode at a center wavelength of 1030 nm.

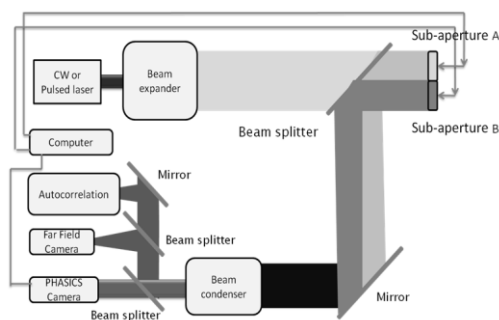


Figure 1 Schematic diagram of the laboratory setup.

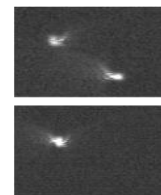


Figure 2 Shows the two spots on the far field camera (top image) when separated and then when brought together (bottom image) in a coherent manner.

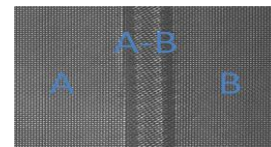


Figure 3 Shows a camera image depicting the three sub apertures. Sub aperture A (primary) and B (secondary) coming from the individual mirrors, with the A-B sub aperture from the interference from the two mirrors.

As shown in Figure 1, the optical layout expands the beam up to 120 mm beam diameter from the laser. It is currently subdivided into two beams by using two mirrors (described as sub-aperture A and B), each 50 mm square. Each sub aperture has independent control of the tip /tilt and Sub aperture A is on a translation stage for control of the piston. There is an actuator for each axis, with a resolution of 30.5 nm and a backlash of  $\sim 6$   $\mu$ m. Each actuator is connected to a computer via a control box. The beam from the two mirrors is imaged relayed to a Wave Front Sensor (WFS) for wavefront analysis. There is a beamsplitter in the path before the WFS so that the beam can go to an 8-bit CCD camera for an image of the far field, as shown in Figure 2. The far field image is useful for two reasons. Firstly, it can act as a starting reference for the position for sub aperture A. Secondly it is used to bring the two far field focuses closely together so that the WFS can then overlap them. The WFS camera and the 8-bit CCD camera are attached to a computer for data retrieval. There is also an autocorrelator (APE) for pulse width measurements, which can be configured to measure interferometric autocorrelation in which the data is taken via a computer from an oscilloscope. The WFS is a PHASICS SID 4 [1] camera which uses the quadriwave lateral shearing

interferometer (QWLSI) method, [2]. This creates an interference pattern between the two wavefronts from the sub apertures and the phase information and piston measurement can be extracted from this pattern, as can be seen in Figure 3. The individual tip and tilt of each mirror is calculated from two further sub aperture either side of the interference of the two beams. These measurements are self referenced, simplifying implementation. It has been shown that the piston measurement accuracy with this system can be is 40 nm or less [2]. Input parameters for the error in the Tip / Tilt and piston are entered into the software and then the program uses these values over the cycle of the program. Values calculated are an average in the readout window of the CCD used in the PHASICS camera, which is typically a few Hz. The closed loop program is written in Lab View which is described in detail in the last annual report [5].

When the parameters of the spatial phasing are met then the pulses temporal characteristics are measured on the autocorrelator. The spatial phase can be seen to below the spatial set parameters but temporal overlap is not always is achieved, this is illustrated in Figure 4, showing the two pulses separated by approximately 1.75 ps. Pulses are temporal combined by the movement of the piston actuator on the sub aperture A. Overlap of the pulses is verified by the measurement of the individual interferometric autocorrelation and also the combination of the two beams as shown in Figure 5. Spatial phase is also measured to confirm that both sup-apertures are also within the set parameters and adjusted accordingly.

Temporal overlap is confirmed by the fact that the maximum amplitude on the sub aperture A and B equate to 1.1 Volts and 0.95 Volts with the combined amplitude maximum measuring 8.1 Volts as shown in Figure 5. These were taken from the oscilloscope with the same voltage and time setting. This is what expected as the amplitude should rise as  $N^2$  [5] where N is the number of apertures, in this case N=2 and therefore the amplitude is seen to increase by a factor of  $\sim 4$  when spatially and temporally overlapped. At the present moment this process is not incorporated into a software loop, but will be implemented in the future.

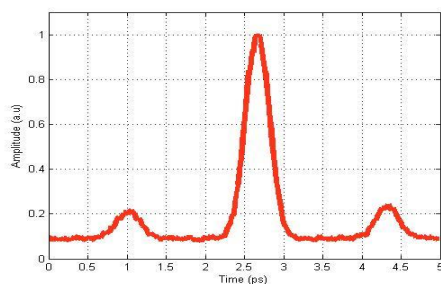


**Figure 4** Autocorrelation measuring the separation of the two pulses by  $\sim 1.7$  ps.

We are able to measure the Strehl ratio of the combined beam with the use of the formulae shown in Equation 1

$$S = e^{-\left(\frac{2\pi\sigma}{\lambda}\right)^2} \quad (1)$$

$\lambda$  = Wavelength of wavefront being measured (nm). The wavelength is 1030 nm.

$\sigma$  = RMS value of wavefront aberrations. (A measured value typically is  $0.1063 \lambda$ )

Using Equation 1 and global RMS measurement of the wavefront we are able to predict a Strehl ratio of 0.64

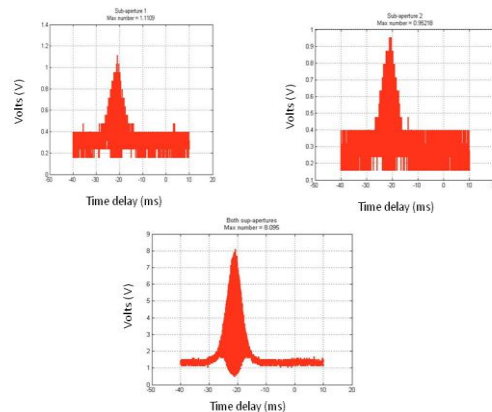


**Figure 5** Interferometric autocorrelation of the individual sub-apertures shown at the top and the temporal overlap of the two sub apertures shown at the bottom, taken with the same voltage and time setting on the oscilloscope monitoring the autocorrelator.

### Conclusions

We have achieved the spatial and temporal overlap of two 50 mm square sub picosecond pulses on our test bed. Temporal overlap of the pulses is not yet incorporated into the loop which monitors the spatial overlap and will be included in the future. We currently are expanding this technique to four apertures and lock them spatial and temporally, using the same WFS. We also plan to implement this technique on the Astra-Gemini beams 7.

### Acknowledgements

This project is funded by the LASERLAB-EUROPE II fund.

### References

1. PHASICS ,A, XTEC Bat 404, Campus de L'Ecole Polytechnique, Route de Saclay 91128, Palaiseau, France
2. S.Mousset, C. Rouyer, G.Marre, N. Blanchot, S. Montant, B. Wattellier, "Piston measurement by quadriwave lateral
3. P.J.Phillips,C. Hernandez-Gomez, I.Musgrave, J.Collier, "Two beam spatial phasing with a CW laser, 2011 Frontiers in Optics Conference Reference num. 1126358,16-20 October, 2011
4. P.J.Phillips,C. Hernandez-Gomez, I.Musgrave, W.Shaikh, J.Collier,"Two beam spatial and temporal phasing with a sub-femtosecond laser", ASSP 2012, Ref. Num. AW4A.10
5. P.J.Phillips,C. Hernandez-Gomez, I.Musgrave, J.Collier, "Two beam spatial phasing with a CW laser", CLF, Annual report 2012
6. G.D Goodno,.et al, "Coherent combination of high power zigzag slab lasers" Optics Letters, Vol.31 , No.9, P1247 2006
7. P J. Hooker, J.L. Collier et al., "The Astra Gemini project-A dual-beam petawatt Ti:Sapphire laser system" J.Phys. IV France 133 (2006) 673-677